SCIENTIFIC REPORTS

OPEN

# A quasi-reagentless point-of-care test for nitrite and unaffected by oxygen and cyanide

Received: 19 October 2018
Accepted: 14 January 2019
Published online: 22 February 2019

Tiago Monteiro[1], Sara Gomes[1], Elena Jubete[2], Larraitz Añorga[2], Célia M. Silveira[1,3] & Maria Gabriela Almeida[1,4]

**The ubiquitous nitrite is a major analyte in the management of human health and environmental risks. The current analytical methods are complex techniques that do not fulfil the need for simple, robust and low-cost tools for on-site monitoring. Electrochemical reductase-based biosensors are presented as a powerful alternative, due to their good analytical performance and miniaturization potential. However, their real-world application is limited by the need of anoxic working conditions, and the standard oxygen removal strategies are incompatible with point-of-care measurements. Instead, a bienzymatic oxygen scavenger system comprising glucose oxidase and catalase can be used to promote anoxic conditions in aired environments. Herein, carbon screen-printed electrodes were modified with cytochrome *c* nitrite reductase together with glucose oxidase and catalase, so that nitrite cathodic detection could be performed by cyclic voltammetry under ambient air. The resulting biosensor displayed good linear response to the analyte (2–200 µM, sensitivity of 326 ± 5 mA $M^{-1}$ $cm^{-2}$ at −0.8 V; 0.8–150 µM, sensitivity of 511 ± 11 mA $M^{-1}$ $cm^{-2}$ at −0.5 V), while being free from oxygen interference and stable up to 1 month. Furthermore, the biosensor's catalytic response was unaffected by the presence of cyanide, a well-known inhibitor of heme-enzymes.**

Nitrite ($NO_2^-$) is an inorganic anion that is found ubiquitously in food, drinking water and the environment, originating from either the biogeochemical nitrogen cycle or from anthropogenic input. Excessive exposure to this anion may present serious risks to public health[1,2] and ecological systems[3]. Therefore, the analytical surveillance of $NO_2^-$ is crucial in the management of health and environmental risks. From a clinical diagnosis perspective, $NO_2^-$ is an important indicator of urinary tract infection (cystitis) due to high levels being present in the urine upon conversion of nitrate by bacterial nitrate reductases[4]. It is also a marker for constitutive oxygen-dependent nitric oxide (NO) synthase activity and endothelial function in humans, with decreased plasma $NO_2^-$ levels being correlated with increasing numbers of cardiovascular risk factors[5,6]. Furthermore, it has been proposed that $NO_2^-$ is a constitute intravascular storage and delivery source of NO, a potent cardioprotective-signalling molecule. This association is of great interest in biomedical research, since administration of $NO_2^-$ could potentially have therapeutic effects in situations where the oxygen-dependent enzymatic production of NO is compromised (i.e. ischemia)[5,7,8].

Most of the existing methods for $NO_2^-$ monitoring[9] are labour-intensive, require expensive laboratory equipment's and/or skilled personnel, and therefore, they cannot fulfil the demand of simple, fast, accurate, low-cost and on-field or point-of-care (POC) detection that the environmental, food and clinical industries need. In this context, electrochemical biosensors based on reductase enzymes are presented as a powerful alternative to the existing methods, due to their fast response time, high selectivity and sensitivity, and miniaturization potential[10]. The multihemic cytochrome *c* nitrite reductase (*cc*NiR) from *Desulfovibrio desulfuricans* ATCC 27774 has been used as the key biorecognition element in the development of such devices[11–15]. This enzyme performs the six-electron reduction of $NO_2^-$ to ammonia and is comprised of a pentahemic catalytic subunit NrfA (61 kDa) bound to a tetrahemic electron donor subunit NrfH (19 kDa), in the proportion of 2NrfA:1NrfH. All hemes are

[1]UCIBIO, REQUIMTE, Faculdade de Ciências e Tecnologia, Universidade NOVA de Lisboa, 2829-516, Monte de Caparica, Portugal. [2]CIDETEC, Sensors Unit, Parque Científico y Tecnológico de San Sebastián, Pº Miramón 196, 2014 Donostia, San Sebastián, Spain. [3]Instituto de Tecnologia Química e Biológica António Xavier, Universidade NOVA de Lisboa, Av. da República, 2780-157, Oeiras, Portugal. [4]Centro de Investigação Interdisciplinar Egas Moniz (CiiEM), Instituto Superior de Ciências da Saúde Egas Moniz, Campus Universitário, Quinta da Granja, 2829-511, Caparica, Portugal. Correspondence and requests for materials should be addressed to M.G.A. (email: mg.almeida@fct.unl.pt)

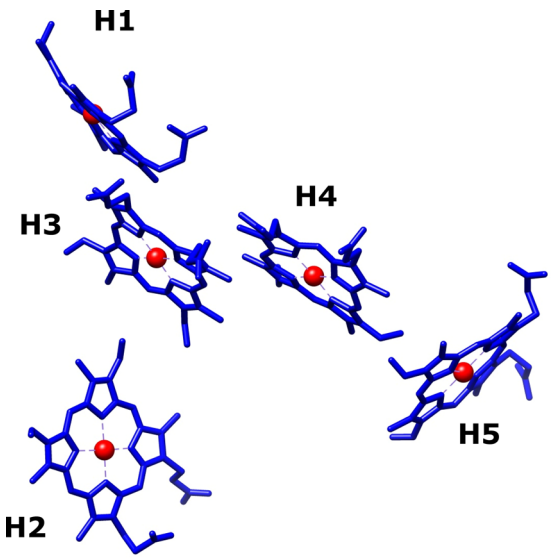


**Figure 1.** Heme groups of the NrfA subunit from *D. desulfuricans* ATCC 2774. Midpoint reduction potentials[17] (*vs* SHE) of the individuals hemes (H) are as follow: H1 −80 mV, H2 −50 mV, H3 −480 mV, H4 −400 mV, H5 + 150 mV. The figure was prepared with the software UCSF Chimera version 1.13.1 using the RCSB PDB entry 1OAH.

*c*-type hexa-coordinated, except for the active centre *c*-heme, which is penta-coordinated with the sixth axial position vacant[16,17]. The hemes in the catalytic subunit exhibit a broad range of reduction potentials, that span from −0.48 to + 0.15 V *vs* SHE (Fig. 1)[17].

Despite their advantages, the real-world application of biosensors based on reductase enzymes is limited by the need of anoxic working conditions. Molecular oxygen ($O_2$) is a main interferent in the analytical process because its reduction to hydrogen peroxide ($H_2O_2$) generates an intense cathodic current that can mask important redox processes that occur at very low potentials (−0.2 and −0.8 V *vs* SHE). This is the case of the catalytic reduction of $NO_2^-$ by *cc*NiR[13–15]. Moreover, $O_2$ can react with redox mediators in their reduced form[18,19] and, in the case of other oxidoreductase-based biosensors, $O_2$ can even compete with them for the enzyme redox co-factors[19].

The standard strategies for $O_2$ removal employed in laboratory settings, such as argon purging or vacuum degassing, are incompatible with on-site monitoring and point-of-care testing. Furthermore, they are not feasible when handling a large number of test samples and can lead to the formation of foam in biological samples. Alternatively, chemical $O_2$ scavengers, such as sodium sulfite[20], can be used to achieve the desired deoxygenation without being cumbersome or compromising the sample's integrity. Nonetheless, it has been reported that *cc*NiR catalyses the reduction of sulfite to sulfide[21], rendering this chemical species incompatible with $NO_2^-$ reductase-based electrochemical biosensing. However, a well-known bienzymatic $O_2$ scavenging system based on the combined action of glucose oxidase (GOx) and catalase (Cat) can be employed to efficiently deoxygenate a sample[22–24]. Both enzymes are free in solution, and upon addition of glucose (the main substrate), $O_2$ is consumed in a two-step cycle. As long as the main substrate is present, and GOx/Cat remain active, any atmospheric $O_2$ that diffuses into the aqueous phase is rapidly scavenged. In this manner, anoxic conditions can be maintained for extended periods of time in an open-air environment in small sample volumes (100–200 µL)[23].

Following this bienzymatic strategy for sample deoxygenation, we have previously developed a miniaturized electrochemical biosensor based on *cc*NiR for the detection of $NO_2^-$ in real samples[15]. The biosensor was capable of operating in anoxic conditions for 1 hour, in an open-air environment. Still, despite the good analytical performance of the device, the GOx and Cat enzymes were employed free in solution. This is unsuitable for a completely reagentless biosensing device and therefore, for its future commercialization. To face this problem, in this paper, we present an improved prototype fabricated by using a very simple co-immobilization procedure of *cc*NiR, GOx and Cat on unmodified carbon screen-printed electrodes (SPEs). The analytical performance and the long-term stability of the new biosensor were evaluated by cyclic voltammetry (CV). Additionally, the catalytic activity of the new biosensor in the presence of cyanide ($CN^-$), a well-known inhibitor of heme-enzymes, like Cat and *cc*NiR[25,26], that can be present in biological fluids due to dietary habits and smoking activities, among other sources[27,28], was also analysed.

By immobilizing the scavenger system together with the *cc*NiR enzyme on SPEs, this work represents a step forward in the establishment of a truly disposable methodology for on-site $NO_2^-$ monitoring. Furthermore, the immobilized scavenger system could also be coupled with other reductases, opening a whole new world of possible POC tests.

## Materials and Methods

**Reagents and solutions.** Glucose, hydrochloric acid and Trizma® were purchased from Sigma-Aldrich. Potassium chloride and sodium nitrite were obtained from VWR. Potassium cyanide was purchased from Merck. All reagents were of analytical grade. Solutions were prepared with deionized water (18 MΩ cm) from a Millipore MilliQ purification system.

GOx (Type II from *Aspergillus niger* 19.3 U $mg^{-1}$) and Cat (from bovine liver, 2–5 kU $mg^{-1}$) were purchased as lyophilized powders from Sigma and solutions were prepared in 100 mM Tris-HCl pH 7.6 buffer, with 100 mM KCl.

*cc*NiR (300 U $mg^{-1}$) was purified from *D. desulfuricans* ATCC 27774 cells, as reported by Almeida and co-workers[17]. The protein concentration was 0.8 mg $mL^{-1}$ in 50 mM phosphate pH 7.6 buffer.

**Biosensors preparation.** The disposable SPEs consisting of a carbon working electrode (WE, $\phi = 4.4$ mm), a carbon counter electrode and a silver/silver chloride (Ag/AgCl) pseudoreference electrode (0.302 V *vs* SHE) were produced at CIDETEC using a Thieme 110E screen-printing machine from Thieme GmbH&Co (Teningen, Germany), an UV tabletop dryer Aktiprint T/A 40-2 from Technigraf (Hessen, Germany) and an oven PN 200 from Carbolite (Derbyshire, UK)[29,30].

The SPEs were used as provided without pre-activation. The WEs were coated with a 5 µL drop of a *cc*NiR solution and air dried for 40 minutes at room temperature (22 ± 2 °C). Afterwards, a 4 µL drop of GOx (187.5 U $mL^{-1}$) and Cat (25 kU $mL^{-1}$) mixture was placed on the *cc*NiR-coated WE and the modified-electrode was air dried for another 40 minutes. The resulting biosensors were stored dry at 4 °C until use.

In the assays where home-made pyrolytic graphite electrodes (PGE) were used instead of SPE, the carbon surface was properly cleaned prior to any modification. The WEs ($\phi = 3$ mm) were polished with alumina 0.3 µm for 2 minutes and then thoroughly rinsed with ethanol 96% (v/v) and deionized water. The electrodes were then sonicated in deionized water for about 5 minutes, being thoroughly rinsed afterwards and dried with an air stream. Once cleaned, the PGEs were covered with a 5 µL drop of a *cc*NiR solution and left to dry for 40 minutes at room temperature. Before placing the WEs in the electrochemical cell, they were rinsed with 100 mM Tris–HCl pH 7.6 buffer containing 100 mM KCl.

**Electrochemical measurements.** All the electrochemical experiments were performed with a PSTAT 12 potentiostat from Autolab (KM Utrecht, The Netherlands), using the software GPES 4.9. A DropSens DSC boxed connector was used to connect the SPE to the potentiostat.

The electrochemical measurements of the SPE-based biosensors were performed by covering the three-electrode system with 50 µL of solutions prepared in the supporting electrolyte (100 mM Tris–HCl pH 7.6 buffer with 100 mM KCl and 80 mM glucose).

For the PGE-based biosensors, the electrochemical measurements were carried out using an Ag/AgCl electrode and Pt wire (both from Radiometer) as reference and counter electrodes, respectively. In addition, the enzymes GOx and Cat were added to 5 mL of the supporting electrolyte in the following final concentrations: 15 U $mL^{-1}$ and 2 kU $mL^{-1}$, respectively.

The CVs were plotted at room temperature (22 ± 2 °C), with a scan rate of 20 mV $s^{-1}$, from −0.1 V to −0.8 V (*vs* reference system). All current values were determined using the analysis software QSoas 1.0[31].

**Cyanide interference.** The performance of the SPE and PGE-based biosensors in the presence of $CN^-$ was assessed by spiking the supporting electrolyte with 10 µM of $NO_2^-$ and afterwards with 10 µM of the interfering compound. A 5 min incubation period (without stirring) was observed between additions. All solutions were prepared in 100 mM Tris-HCl pH 7.6 buffer, with 100 mM KCl.

The catalytic currents ($\Delta I_{cat}$) were determined at the cathodic peak (ca. −0.4 V); all values were corrected for the non-catalytic current measured in the absence of $NO_2^-$. The relative catalytic response (Equation 1) was calculated as:

$$Relative\ Catalytic\ Response\ (\%) = \frac{\Delta I_{cat\ NO_2^-\ \&\ CN^-}}{\Delta I_{cat\ NO_2^-}} \times 100 \quad (1)$$

Controls were performed by spiking the supporting electrolyte (containing $NO_2^-$) with equal volumes of buffer solution. All assays were replicated three times ($n = 3$).

**Analytical performance – sensitivity, stability and reproducibility.** The sensitivity (slope of the calibration curve) of the SPE-based biosensor was determined by measuring the response to different $NO_2^-$ standard solutions (one electrode per standard), with concentrations ranging from 0.8 to 200 µM. A 5 min incubation period was observed before recording the CV. The $\Delta I_{cat}$ values were determined at −0.5 V and −0.8 V and plotted *vs* the analyte concentrations. Each assay was replicated three times ($n = 3$).

The SPE-based biosensor's long-term stability was evaluated for 1 month. A batch of biosensors was prepared as previously described and stored dry at 4 °C when not in use. On the first day, 6 single-use biosensors were used to measure the initial response to a 50 µM $NO_2^-$ standard solution. Afterwards, the measurements were repeated 3 times every five days, up to 30 days.

The reproducibility was determined by calculating the relative standard deviation (RSD) of the $\Delta I_{cat}$ of 10 SPE-based biosensors to 50 µM $NO_2^-$.

**Real sample analysis.** Urine was collected from a healthy male volunteer (with informed consent) 4 hours after the first morning evacuation using a clean plastic vial and no pre-treatment was performed. The pH was

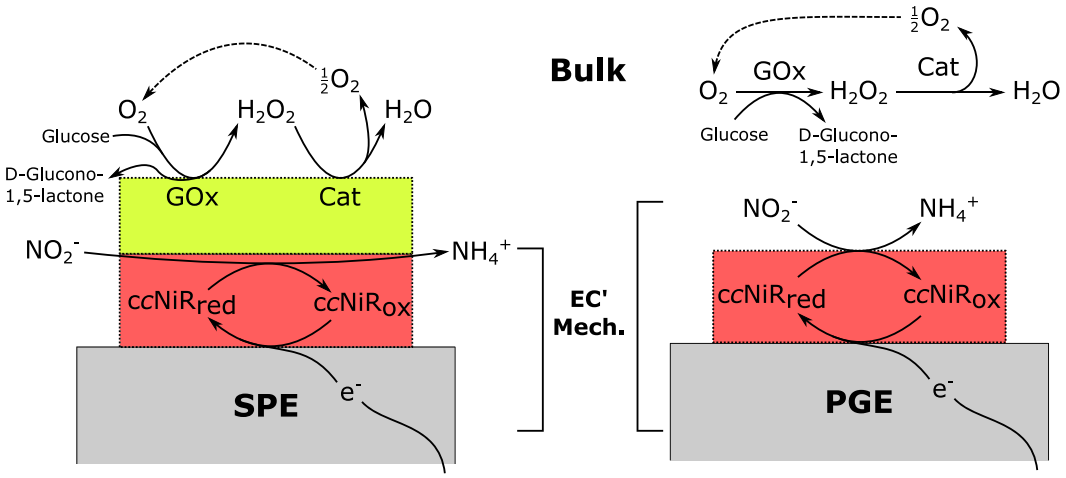


**Figure 2.** Schematic representation of the *cc*NiR/GOx/Cat-modified SPE and *cc*NiR-modified PGE, with GOx and Cat in solution. *EC' Mech*. stands for the catalytic reaction mechanism where *cc*NiR is first reduced ($cc\text{NiR}_{red}$) by the WE in the electrochemical reaction (E), and afterwards it is reoxidized ($cc\text{NiR}_{ox}$) in the chemical reaction (C') with $NO_2^-$.

measured using a 210 Benchtop pH/mV meter (Bante Instruments). Immediately prior to the analysis, 820 µL of urine were supplemented with 80 µL of glucose (1 M) and 100 µL of $NO_2^-$ standard (0–2 mM) prepared in distilled water. Afterwards, 50 µL of the mix were placed on the SPE-based biosensors and a 5 min incubation period was observed before recording the CV. Each assay was replicated three times ($n = 3$).

## Results and Discussion

**Immobilization of the oxygen scavenger system.** In our previous work[15], the GOx/Cat $O_2$ scavenger system was successfully employed to remove dissolved $O_2$ from the supporting electrolyte, maintaining anoxic conditions in the electrochemical cells. Since *cc*NiR was immobilized on the surface of carbon SPE, the analyte detection was easily achieved by spiking the supporting electrolyte with $NO_2^-$ solutions and recording the corresponding $\Delta I_{cat}$ increase by CV. However, the reported system required the addition of the GOx and Cat enzymes to a relatively high working volume (5 mL) of supporting electrolyte, increasing the overall cost of the assay. To face these problems, a new prototype has been developed in which the GOx and Cat are immobilized together with the *cc*NiR on the SPE and the volume of the supporting electrolyte is reduced down to 50 µL. To ensure direct electron transfer between the WE and *cc*NiR, the enzyme needs to be in contact with the surface of the electrode[10,32]. For this reason, the sensing layer (where $NO_2^-$ reduction occurs) was the first to be adsorbed on the electrode surface, followed by the immobilization of the GOx/Cat layer, as schematized in Fig. 2 for the SPE.

To analyse the ability of the GOx and Cat enzymes to promote anoxic conditions in an aerated environment once immobilized, the electrodes were modified with both enzymes but without *cc*NiR. The resulting GOx/Cat-modified SPEs were covered with 50 µL of the supporting electrolyte and characterized by CV. As shown in Fig. 3, in the absence of glucose, a broad cathodic wave is observed due to the electrochemical reduction of dissolved $O_2$ in the supporting electrolyte. After adding glucose to the electrolyte, the cathodic current attributed to $O_2$ reduction drastically decreases. This is due to glucose being oxidized by GOx, while the co-substrate $O_2$ (electron acceptor) is reduced to $H_2O_2$. The latter is then dismutated by Cat into $O_2$ and water (Fig. 2). Despite $O_2$ regeneration at the end of the cycle, for each iteration, the total amount of the co-substrate is reduced by a factor of 2[23]. Owing to the high turnover numbers of GOx and Cat, after a few cycles, the $O_2$ content quickly drops below the detection limit, and the background current remains stable for one hour (cf. Fig. 3, inset). The results obtained are comparable to those reported in previous works[15,23], where GOx and Cat were used free in the supporting electrolyte. Hence, the immobilization of both enzymes on a carbon SPE does not compromise their bioactivity.

**Cyanide interference.** $CN^-$ is a well-known inhibitor of heme-enzymes[25,26] and its effect on the biosensor's catalytic response was measured in the presence of equimolar concentration of $NO_2^-$. Figure 4 shows the CVs obtained for the assays with *cc*NiR/GOx/Cat-modified SPE and, for comparison, the ones obtained for the *cc*NiR-modified PGE (in which the GOx and Cat were added to the supporting electrolyte). In both cases, upon the addition of $NO_2^-$, a well-defined cathodic peak was obtained around −0.4 V ($NO_2^-$ bioelectroreduction). This was due to the direct electron transfer between *cc*NiR and the WE surface, coupled with the enzyme catalysed 6 electron reduction reaction of $NO_2^-$ to ammonia, according to a catalytic (EC') mechanism, in which a reversible electron transfer reaction is followed by an irreversible chemical reaction (Fig. 2)[10,33,34].

In the presence of $CN^-$, the cathodic peak current obtained for the *cc*NiR-modified PGE showed a drastic decrease bellow the non-catalytic current, accompanied by a + 90 mV shift in the peak potential. A similar shift (+70 mV) was observed in non-turnover conditions for the *cc*NiR from *Shewanella oneidensis*, which was attributed to the binding of the ligand to the penta-coordinated catalytic heme[35]. It was also reported that the binding event of $CN^-$ to the *cc*NiR from *Escherichia coli* resulted in a decrease in catalytic current and a displacement of the peak potential towards more positive values[26]. A more drastic reduction potential shift was observed in

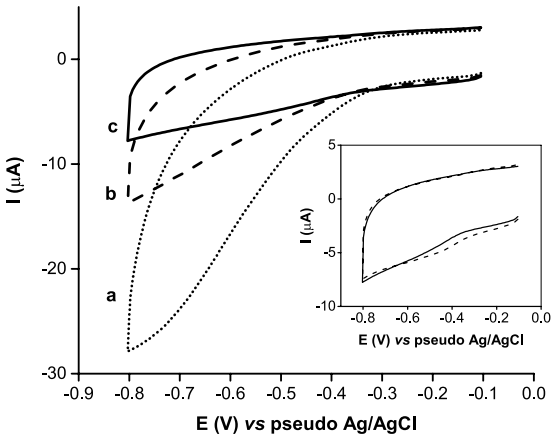


**Figure 3.** CVs of the GOx and Cat-modified carbon SPEs: (**a**) background current recorded in the supporting electrolyte without glucose ($O_2$ is present); (**b**) background current recorded after spiking the supporting electrolyte with 80 mM glucose ($t_0$ min); (**c**) background current recorded in the supporting electrolyte containing 80 mM glucose after 5 min. Inset: background current after (line) 5 and (dash) 60 minutes.

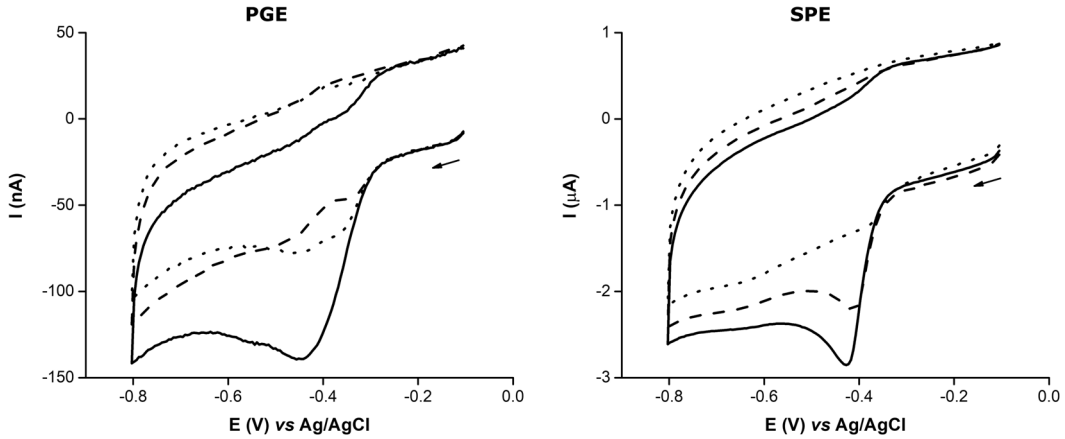


**Figure 4.** CVs obtained for the *cc*NiR-modified PGE (GOx and Cat in solution) and *cc*NiR/GOx/Cat-modified SPE in the presence of 10 μM $NO_2^-$ before (—) and after (**- - -**) adding 10 μM $CN^-$ to the solution. The non-catalytic (···) current (without $NO_2^-$/$CN^-$ in solution) for each electrode is also shown. Supporting electrolyte 100 mM Tris-HCl (pH 7.6) with 100 mM KCl and 80 mM glucose; scan rate 20 mV $s^{-1}$.

the presence of carbon monoxide (another inhibitor of *cc*NiR), where the binding event resulted in the dislodgment of the catalytic heme reduction potential to outside of the voltammogram envelop[36]. Therefore, the binding of $CN^-$ to several of the heme groups from the *cc*NiR complex (see Fig. 1), particularly to the catalytic heme, could be shifting its reduction potential outside the range of applied potentials, explaining why the cathodic peak around −0.4 V was smaller than the one observed in the non-catalytic voltammogram. However, for the modified SPE, the decrease of the cathodic peak current and shift in peak potential (+10 mV) were far smaller. Considering the addition of equal volumes of $CN^-$ or buffer (control) solutions caused a similar decrease in current response (about 50%; see Fig. 5), we conclude that this was due to the dilution of $NO_2^-$ and, therefore no inhibitory effects of $CN^-$ were observed on the SPE based biosensor. Note that for the modified PGE, the catalytic response decreased 15% due to $NO_2^-$ dilution, but the enzyme was completely inhibited upon addition of $CN^-$, since the relative catalytic response decreased 120%. This value resulted from the current response in the presence of the inhibitor being smaller than the initial non-catalytic current, as observed in Fig. 4.

Why *cc*NiR was not effectively inhibited when it was immobilized on the SPE is not clear, but could be due to several reasons: (i) $CN^-$ adsorption by the carbon paste of the SPE; (ii) $CN^-$ binding to the Cat enzyme; (iii) the formation of glucose-cyanohydrin. Firstly, the carbon ink used in the fabrication of the SPE could produce a unique environment that prevented the inhibitor from successfully binding to the $NO_2^-$ reductase active site. Activated carbon has been shown to adsorb $CN^-$[37]; the ink used in the fabrication of the printed working and counter electrodes might behave as activated carbon, adsorbing $CN^-$ to some extent. Secondly, Cat could be scavenging $CN^-$, since the latter binds to the active site of the enzyme[25]. Thus, the inhibitor that reached the *cc*NiR layer on the SPE could be insufficient to effectively block its activity. However, enzyme inhibition was observed in the PGE assay, where the Cat/$CN^-$ ratio was kept the same; so the hypothesis of Cat acting as a $CN^-$ scavenger seems unlikely. Finally, the glucose present in the support electrolyte could be acting as a $CN^-$ scavenger,

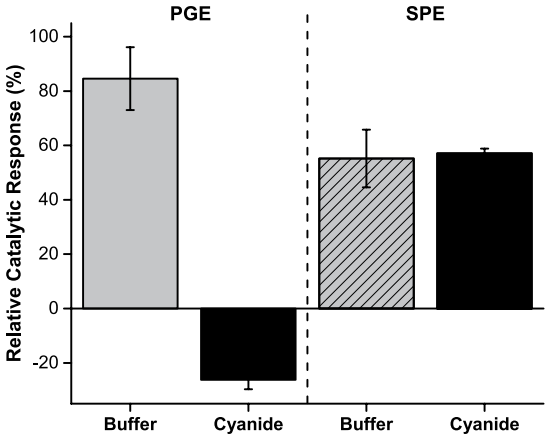


**Figure 5.** Relative catalytic response of the PGE and SPE-based biosensors to $CN^-$ interference ($n = 3$). $NO_2^-$ was previously added to the supporting electrolyte; the analyte-interferent ratio was 1:1. Control was performed by spiking the supporting electrolyte with a $CN^-$ free buffer solution.

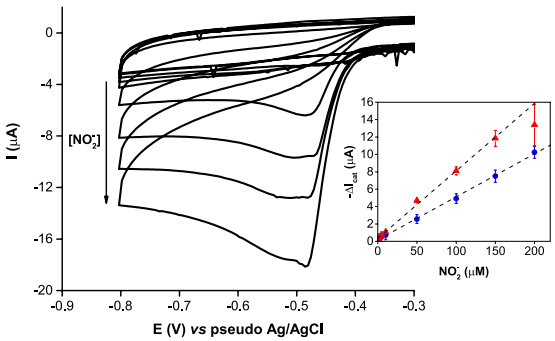


**Figure 6.** CVs of the SPE-based biosensors response to $NO_2^-$ standard solutions (0.8–200 µM) containing 80 mM glucose. Measurements ($n = 3$) were performed in an open-air environment. Inset: linear correlation between the $\Delta I_{cat}$ at either (▲) −0.5 V (slope 511 mA $M^{-1}$ $cm^{-2}$, $R^2$ 0.998) or (●) −0.8 V (slope 326 mA $M^{-1}$ $cm^{-2}$, $R^2$ 0.999) and $NO_2^-$ concentration. The supporting electrolyte was 100 mM Tris-HCl (pH 7.6) with 100 mM KCl and 80 mM glucose; scan rate 20 mV $s^{-1}$.

producing glucose-cyanohydrin[38]. However, this possibility was ruled out, as this was not observed in the assays with the PGE. Therefore, the *cc*NiR enzyme was shielded from inhibition probably due to the adsorption of $CN^-$ by the carbon surfaces of the SPE.

Worth of mention, no $O_2$ or $H_2O_2$ interferences were observed on the CVs after spiking the electrolyte with $CN^-$, which means that the immobilized GOx and Cat remained active in the presence of $CN^-$. Since no inhibition in reductase and catalase activities were observed when using the SPE as immobilization surface, it is reasonable to say that this system could be used with other heme-proteins based biosensing applications, such as other cytochromes and hemoglobins.

**Nitrite detection.** The analyte detection was carried out by covering the SPE-based biosensors with a 50 µL drop of $NO_2^-$ standard solutions (0.8–200 µM) containing glucose, and giving a 5 min incubation time for the scavenger system to remove the dissolved $O_2$; CVs were then recorded and the current was measured at the inversion potential −0.8 V (Fig. 6). The increase in $NO_2^-$ concentration resulted in increased cathodic peak currents, according to the EC' mechanism (see previous section). The $\Delta I_{cat}$ varied linearly with $NO_2^-$ concentration in the range of 2–200 µM, with a sensitivity of 326 ± 5 mA $M^{-1}$ $cm^{-2}$ (Fig. 6, inset). The limit of detection (LOD) was estimated to be 4.7 µM, using the standard definition $3S_a/m$, where $S_a$ is the standard deviation of the *y*-intercept and *m* is the slope of the calibration curve.

The sensitivity of the presented biosensor is 35% lower than the one reported in our previous work with *cc*NiR-modified SPE biosensors (550 mA $M^{-1}$ $cm^{-2}$ at −0.8 V working potential)[15]. We attribute the lowered performance to the differences in electrode preparation, namely the absence of carbon conductive ink in the enzyme mixture applied on the WE, and the presence of a protein (GOx/Cat) coat that could be acting as a diffusion barrier to the analyte, thereby lowering the current response. Nevertheless, the analytical features displayed by the biosensor are suitable to monitor $NO_2^-$ in drinking waters according to the guidelines from the World Health Organization (3 ppm or 65 µM)[39] and the United States Environmental Protection Agency (1 ppm or 22 µM)[40]. In what concerns the European Union directives, the LOD is slightly higher than the maximum permitted value (0.1 ppm or 2 µM)[41].

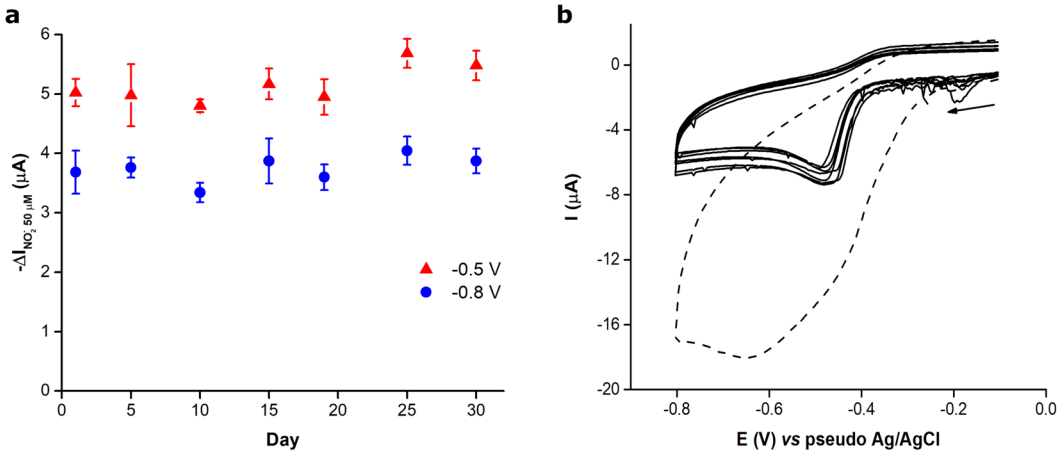


**Figure 7.** (**a**) Long-term storage stability of a single batch of biosensors recorded over a period of 30 days. Each point represents the average current at (▲) −0.5 V or (●) −0.8 V for a 50 µM $NO_2^-$ standard solution (first day $n = 6$; following days $n = 3$). (**b**) Average uncorrected CVs of the SPE-based biosensors' response to (—) 50 µM $NO_2^-$ standard solution and (- - -) to a blank solution without $NO_2^-$ or glucose. The intense cathodic peak near −0.6 V corresponds to the reduction of dissolved $O_2$. The supporting electrolyte was 100 mM Tris-HCl (pH 7.6) with 100 mM KCl; scan rate 20 mV $s^{-1}$.

| $NO_2^-$ added (µM) | $NO_2^-$ found (µM) | | Recovery (%) | |
|---|---|---|---|---|
| | −0.5 V | −0.8 V | −0.5 V | −0.8 V |
| 5 | 5 ± 2 | 5 ± 1 | 101 ± 31 | 104 ± 23 |
| 50 | 50 ± 2 | 48 ± 5 | 99 ± 5 | 96 ± 9 |
| 100 | 82 ± 7 | 99 ± 5 | 82 ± 7 | 99 ± 5 |

**Table 1.** Recovery percentages for $NO_2^-$ in urine using the SPE-based biosensor.

Alternatively, the detection of $NO_2^-$ could be performed as well at a less negative potential such as −0.5 V, where the sensitivity was higher (511 ± 11 mA $M^{-1}$ $cm^{-2}$) for a $NO_2^-$ concentration between 0.8 and 150 µM (Fig. 6, inset), with a similar LOD (4.5 µM). Worth mentioning, although the upper limit of the linear range decreased at this working potential, the lower limit was improved.

Another improvement of the new the biosensor configuration to the previous work was the higher reproducibility: RSD 8% at −0.8 V or 4% at −0.5 V ($n = 10$) compared to RSD 20%[15].

**Storage stability.** The long-term storage stability of the developed biosensor was tested over a period of 1 month. To this aim, a batch of single-use biosensors was prepared (those not in use were stored in dry conditions at 4 °C) and the catalytic response to 50 µM $NO_2^-$ was recorded every five days and compared with the one measured on the first day – see Fig. 7a. During this time, the biosensor's response was considered stable since no consecutive decrease in the $\Delta I_{cat}$ was observed, at either −0.5 V or −0.8 V. In Fig. 7b, the average CVs measured in each day are compared with a control bioelectrode (dashed line) tested in electrolyte that did not contain glucose or the analyte. The intense reduction signal of $O_2$ observed at −0.6 V in the control is clearly absent from all other CVs, which suggests that the enzymes responsible for removing the dissolved $O_2$ from the supporting electrolyte also remain active for 1 month.

**Real sample analysis.** Urine (pH 6.75) was selected as the real complex matrix to evaluate the practical application of the proposed SPE-based biosensor in the determination of $NO_2^-$. The biological sample was collected and analysed in the day of the experiments, without any pretreatment. The samples were supplemented with 80 mM glucose and increasing $NO_2^-$ concentrations (0–200 µM). The obtained calibration curve was used to calculate the concentration of the analyte in the real samples. The recovery percentages (Table 1) for the concentrations of 5, 50 and 100 µM were in the range 96–104% when measurements were performed at −0.8 V. These results show that the proposed biosensor could be effectively employed in the determination of $NO_2^-$ in real urine samples where the analyte's levels have been reported to be up to 400 µM in the case of confirmed bacteriuria[4].

**Comparison with other miniaturized devices for nitrite determination.** The analytical features of the SPE-based biosensor herein presented are summarized in Table 2 and compared with other miniaturized devices developed to monitor $NO_2^-$. Overall, the proposed biosensor performed similarly to the other mentioned analytical tools. Several of these devices are colourimetric paper-based[42–46] tests, reflecting the current trend of using cellulose materials as substrates for the development of low-cost and sustainable POC assays[47,48]. However, the detection method is mainly based on the Griess reaction[49], which is rather slow (10–20 min) and prone to

| Device | Detection | LR (µM) | LOD (µM) | RSD (%) | Storage Stability | RT (min) | Ref. |
|---|---|---|---|---|---|---|---|
| µPAD | Colourimetric (Griess reaction) | Up to 25 | 5.6 | — | 12 h at 25 °C (protected from light) | 15 | 42 |
| µPAD | Colourimetric (Griess reaction) | 87–1800 | 11.3 | — | — | 15 | 43 |
| µPAD | Colourimetric (Griess reaction) | 10–150 | 1.0 | 2.9 | 1 month at −20 °C (under vacuum) | 5 | 44 |
| µPAD | Colourimetric (Griess reaction) | 0.7–145 | 0.43 | 6.5 | — | 10 | 45 |
| µPAD | Colourimetric (dihydrotetrazine) | 5–500 | 1.3 | 3.5–4.7 | 3 weeks at 4 °C (protected from light) | 5 | 46 |
| SPE modified with AgMCs-PPA/PVA | Flow injection amperometry (+0.7 V[a]) | 2–800 | 4.5 | <6 | — | — | 53 |
| SPE modified with C*c*R nanostructured layer | Cyclic voltammetry (+0.8 V[a]) | 0.1–1600 | 0.06 | 3.8 | 3 weeks at 4 °C | — | 54 |
| SPE modified with MWCNTs | Batch injection amperometry (+0.7 V[a]) | 1–500 | 0.06 | 1.1 | — | — | 55 |
| Wireless microfluidic analytical platform | Colourimetric (Griess reaction) | Up to 17 | 0.49 | 1.93 | — | 20 | 56 |
| SPE modified with *cc*NiR/GOx&Cat | CV (−0.5/−0.8 V[a]) | 0.8/2–150/200 | 4.5/4.7 | 4/8 | 1 month at 4 °C | 5 | This work |

**Table 2.** Comparison of miniaturized analytical devices for the determination of $NO_2^-$. AgNP-PPA/PVA – silver microcubics-polyacrylic acid/poly vinyl alcohol; *cc*NiR/GOx&Cat – cytochrome *c* nitrite reductase, glucose oxidase and catalase; C*c*R – cytochrome *c* reductase; CV – cyclic voltammetry; LOD – limit of detection; LR – linear range; MWCNTs – multi-walled carbon nanotubes; RSD – relative standard deviation; RT – response time; SPE – screen-printed electrode; µPAD – microfluidic paper-based analytical device. [a]*versus* Ag/AgCl pseudoreference.

interference when used in real samples[9,50–52], that can only be eliminated by adding a pretreatment step[51,52]. Additionally, special storage conditions (see Table 2) are required to assure the stability of the reactants that are susceptible to photobleaching[43]. The other devices are SPE-based[53–55] and rely on the oxidation of $NO_2^-$ at high overpotentials, where the oxidation of other common biological molecules could be a source of interference in the analytical assay[52]. Furthermore, some of these devices require complex and high-cost additional components, such as pumps and automatic injectors[53,55,56], which increase the cost of implementation of the method.

The SPE-biosensor proposed in this work uses a simple and straightforward measurement protocol, without any sample pretreatment, thus being user-friendly and achieving a measurable signal in a short time. Although the device's substrate is not paper-based, it is made of a thin sheet of plastic material, as opposed to the standard commercially available ceramic SPE, allowing an estimated cost of 0.70 € per biosensor unit.

## Conclusions

In this work, a simple and low-cost procedure for the co-immobilization of an enzymatic $O_2$ scavenger system (GOx and Cat) and *cc*NiR (the biosensing element) on a bare carbon SPE was presented. The resulting biosensor was developed for monitoring the enzymatic reduction of $NO_2^-$ in open-air working conditions, without the interference of oxygen. The enzymes GOx and Cat retained their bioactivity upon immobilization, removing dissolved molecular oxygen content from the drop of supporting electrolyte placed on top of the electrode chip, for at least 1 hour. The immobilization of all three enzymes on one electrode allowed for a significant reduction of the work volume required for each measurement, and for a much more practical working procedure, since the need for conventional glass cells and cumbersome oxygen purging methods was eliminated. In terms of analytical performance, the resulting biosensor responded linearly to $NO_2^-$ in the concentration range from 0.8 to 200 µM, with good sensitivity and reproducibility (RSD 4–8%), being well suited for the monitoring of $NO_2^-$ in drinking waters according to international guidelines, and in the analysis of urine in clinical settings. Also, all three immobilized enzymes remained active for at least 1 month.

When *cc*NiR was immobilized on the SPE, interference from $CN^-$ (heme-protein inhibitor) on the biosensor's catalytic response was found to be negligible. Furthermore, the catalase activity was not compromised since no $H_2O_2$ formation was detected. However, with PGE as the immobilization surface, the $NO_2^-$ reductase activity was inhibited in the presence of $CN^-$. The carbon ink used for the fabrication of the SPE working and counter electrodes might produce a unique environment for the immobilization of heme proteins, shielding them from $CN^-$ inhibition.

This work represents a step forward in the establishment of a truly disposable methodology for low-cost (0,70€ per unit), disposable, on-site $NO_2^-$ biosensing. Furthermore, the immobilized oxygen scavenger system could also be coupled with other reductases, opening a whole new world of possible disposable devices for POC testing where oxygen is a major interferent.

## References


1. Hord, N. G., Tang, Y. & Bryan, N. S. Food sources of nitrates and nitrites: the physiologic context for potential health benefits. *Am. J. Clin. Nutr.* **90**, 1–10 (2009).
2. Habermeyer, M. *et al*. Nitrate and nitrite in the diet: How to assess their benefit and risk for human health. *Mol. Nutr. Food Res.* **59**, 106–128 (2015).
3. Camargo, J. A. & Alonso, Á. Ecological and toxicological effects of inorganic nitrogen pollution in aquatic ecosystems: A global assessment. *Environ. Int.* **32**, 831–849 (2006).
4. Lundberg, J. O. N. *et al*. Urinary nitrite: More than a marker of infection. *Urology* **50**, 189–191 (1997).

5. Dejam, A., Hunter, C. J., Schechter, A. N. & Gladwin, M. T. Emerging role of nitrite in human biology. *Blood Cells. Mol. Dis.* **32**, 423–429 (2004).
6. Kleinbongard, P. *et al*. Plasma nitrite concentrations reflect the degree of endothelial dysfunction in humans. *Free Radic. Biol. Med.* **40**, 295–302 (2006).
7. Bryan, N. S. *et al*. Dietary nitrite supplementation protects against myocardial ischemia-reperfusion injury. *Proc. Natl. Acad. Sci. USA* **104**, 19144–19149 (2007).
8. Lundberg, J. O. *et al*. Nitrate and nitrite in biology, nutrition and therapeutics. *Nat. Chem. Biol.* **5**, 865–869 (2009).
9. Wang, Q.-H. *et al*. Methods for the detection and determination of nitrite and nitrate: A review. *Talanta* **165**, 709–720 (2017).
10. Almeida, M. G., Serra, A., Silveira, C. M. & Moura, J. J. G. Nitrite Biosensing via Selective Enzymes – A Long but Promising Route. *Sensors* **10**, 11530–11555 (2010).
11. Da Silva, S., Cosnier, S., Almeida, M. G. & Moura, J. J. G. An efficient poly(pyrrole-viologen)-nitrite reductase biosensor for the mediated detection of nitrite. *Electrochem. commun.* **6**, 404–408 (2004).
12. Chen, H. *et al*. Highly sensitive nitrite biosensor based on the electrical wiring of nitrite reductase by [ZnCr-AQS] LDH. *Electrochem. commun.* **9**, 2240–2245 (2007).
13. Silveira, C. M. *et al*. An efficient non-mediated amperometric biosensor for nitrite determination. *Biosens. Bioelectron.* **25**, 2026–2032 (2010).
14. Silveira, C. M. *et al*. Enhanced Direct Electron Transfer of a Multihemic Nitrite Reductase on Single-walled Carbon Nanotube Modified Electrodes. *Electroanalysis* **22**, 2973–2978 (2010).
15. Monteiro, T. *et al*. Construction of effective disposable biosensors for point of care testing of nitrite. *Talanta* **142**, 246–251 (2015).
16. Cunha, C. A. *et al*. Cytochrome c nitrite reductase from Desulfovibrio desulfuricans ATCC 27774. The relevance of the two calcium sites in the structure of the catalytic subunit (NrfA). *J. Biol. Chem.* **278**, 17455–17465 (2003).
17. Almeida, M. G. *et al*. The isolation and characterization of cytochrome c nitrite reductase subunits (NrfA and NrfH) from Desulfovibrio desulfuricans ATCC 27774. *Eur. J. Biochem.* **270**, 3904–3915 (2003).
18. Bird, C. L. & Kuhn, A. T. Electrochemistry of the viologens. *Chem. Soc. Rev.* **10**, 49–82 (1981).
19. Prévoteau, A. & Mano, N. Oxygen reduction on redox mediators may affect glucose biosensors based on "wired" enzymes. *Electrochim. Acta* **68**, 128–133 (2012).
20. Quan, D. *et al*. Electrochemical Determination of Nitrate with Nitrate Reductase-Immobilized Electrodes under Ambient Air. *Anal. Chem.* **77**, 4467–4473 (2005).
21. Pereira, I. C., Abreu, I. A., Xavier, A. V., LeGall, J. & Teixeira, M. Nitrite Reductase from Desulfovibrio desulfuricans (ATCC 27774) – A Heterooligomer Heme Protein with Sulfite Reductase Activity. *Biochem. Biophys. Res. Commun.* **224**, 611–618 (1996).
22. Harada, Y., Sakurada, K., Aoki, T., Thomas, D. D. & Yanagida, T. Mechanochemical coupling in actomyosin energy transduction studied by *in vitro* movement assay. *J. Mol. Biol.* **216**, 49–68 (1990).
23. Plumeré, N., Henig, J. & Campbell, W. H. Enzyme-catalyzed O2 removal system for electrochemical analysis under ambient air: application in an amperometric nitrate biosensor. *Anal. Chem.* **84**, 2141–2146 (2012).
24. Efimov, I. *et al*. A simple method for the determination of reduction potentials in heme proteins. *FEBS Lett.* **588**, 701–704 (2014).
25. Ogura, Y. & Yamazaki, I. Steady-state kinetics of the catalase reaction in the presence of cyanide. *J. Biochem.* **94**, 403–408 (1983).
26. Gwyer, J. D., Richardson, D. J. & Butt, J. N. Resolving complexity in the interactions of redox enzymes and their inhibitors: Contrasting mechanisms for the inhibition of a cytochrome c nitrite reductase revealed by protein film voltammetry. *Biochemistry* **43**, 15086–15094 (2004).
27. Ma, J. & Dasgupta, P. K. Recent developments in cyanide detection: A review. *Anal. Chim. Acta* **673**, 117–125 (2010).
28. Jaszczak, E., Narkowicz, S., Namieśnik, J. & Polkowska, Ż. Determination of cyanide in urine and saliva samples by ion chromatography with pulsed amperometric detection. *Monatshefte für Chemie - Chem. Mon.* **148**, 1645–1649 (2017).
29. Lamas-Ardisana, P. J. *et al*. Disposable amperometric biosensor based on lactate oxidase immobilised on platinum nanoparticle-decorated carbon nanofiber and poly(diallyldimethylammonium chloride) films. *Biosens. Bioelectron.* **56**, 345–351 (2014).
30. Loaiza, O. A. *et al*. Graphitized carbon nanofiber-Pt nanoparticle hybrids as sensitive tool for preparation of screen printing biosensors. Detection of lactate in wines and ciders. *Bioelectrochemistry* **101**, 58–65 (2015).
31. Fourmond, V. QSoas: A Versatile Software for Data Analysis. *Anal. Chem.* **88**, 5050–5052 (2016).
32. Habermüller, K., Mosbach, M. & Schuhmann, W. Electron-transfer mechanisms in amperometric biosensors. *Fresenius. J. Anal. Chem.* **366**, 560–568 (2000).
33. Lojou, É. & Bianco, P. Application of the electrochemical concepts and techniques to amperometric biosensor devices. *J. Electroceramics* **16**, 79–91 (2006).
34. Serra, A. S. *et al*. Cooperative use of cytochrome cd1 nitrite reductase and its redox partner cytochrome c552 to improve the selectivity of nitrite biosensing. *Anal. Chim. Acta* **693**, 41–46 (2011).
35. Stein, N. *et al*. Correlations between the Electronic Properties of Shewanella oneidensis Cytochrome c Nitrite Reductase (ccNiR) and Its Structure: Effects of Heme Oxidation State and Active Site Ligation. *Biochemistry* **54**, 3749–3758 (2015).
36. Almeida, M. G. *et al*. A needle in a haystack: the active site of the membrane-bound complex cytochrome c nitrite reductase. *FEBS Lett.* **581**, 284–288 (2007).
37. Stavropoulos, G. G., Skodras, G. S. & Papadimitriou, K. G. Effect of solution chemistry on cyanide adsorption in activated carbon. *Appl. Therm. Eng.* **74**, 182–185 (2015).
38. Lewandowski, Z. Biological denitrification in the presence of cyanide. *Water Res.* **18**, 289–297 (1984).
39. World Health Organization. Chemical contaminants in drinking-water. In Guidelines for drinking-water quality: fourth edition incorporating the first addendum 398–403 (2017).
40. EPA. National Primary Drinking Water Regulations Complete Table. **7** (2009).
41. European Commission. Council Directive 98/83/EC of 3 November 1998 on the quality of water intended for human consumption. *Off. J. Eur. Communities L* **330**, 32–54 (1998).
42. Cardoso, T. M. G., Garcia, P. T. & Coltro, W. K. T. Colorimetric determination of nitrite in clinical, food and environmental samples using microfluidic devices stamped in paper platforms. *Anal. Methods* **7**, 7311–7317 (2015).
43. Lopez-Ruiz, N. *et al*. Smartphone-Based Simultaneous pH and Nitrite Colorimetric Determination for Paper Microfluidic Devices. *Anal. Chem.* **86**, 9554–9562 (2014).
44. Jayawardane, B. M., Wei, S., McKelvie, I. D. & Kolev, S. D. Microfluidic Paper-Based Analytical Device for the Determination of Nitrite and Nitrate. *Anal. Chem.* **86**, 7274–7279 (2014).
45. Vidal, E., Lorenzetti, A. S., Lista, A. G. & Domini, C. E. Micropaper-based analytical device (μPAD) for the simultaneous determination of nitrite and fluoride using a smartphone. *Microchem. J.* **143**, 467–473 (2018).
46. Ortiz-Gomez, I. *et al*. Tetrazine-based chemistry for nitrite determination in a paper microfluidic device. *Talanta* **160**, 721–728 (2016).
47. Silveira, C., Monteiro, T. & Almeida, M. Biosensing with Paper-Based Miniaturized Printed Electrodes–A Modern Trend. *Biosensors* **6**, 51 (2016).
48. Cate, D. M., Adkins, Ja, Mettakoonpitak, J. & Henry, C. S. Recent Developments in Paper-Based Microfluidic Devices. *Anal. Chem.* **87**, 19–41 (2015).
49. Ellis, G., Adatia, I., Yazdanpanah, M. & Makela, S. K. Nitrite and Nitrate Analyses: A Clinical Biochemistry Perspective. *Clin. Biochem.* **31**, 195–220 (1998).

50. Kleinbongard, P., Rassaf, T., Dejam, A., Kerber, S. & Kelm, M. Griess method for nitrite measurement of aqueous and protein-containing samples. *Methods Enzymol.* **359**, 158–68 (2002).
51. Sun, J., Zhang, X., Broderick, M. & Fein, H. Measurement of Nitric Oxide Production in Biological Systems by Using Griess Reaction Assay. *Sensors* **3**, 276–284 (2003).
52. Bellavia, L., Kim-Shapiro, D. B. & King, S. B. Detecting and monitoring NO, SNO and nitrite *in vivo*. *Futur. Sci. OA* **1**, 229–262 (2015).
53. Promsuwan, K., Thavarungkul, P., Kanatharana, P. & Limbut, W. Flow injection amperometric nitrite sensor based on silver microcubics-poly (acrylic acid)/poly (vinyl alcohol) modified screen printed carbon electrode. *Electrochim. Acta* **232**, 357–369 (2017).
54. Santharaman, P. *et al*. ARM-microcontroller based portable nitrite electrochemical analyzer using cytochrome c reductase biofunctionalized onto screen printed carbon electrode. *Biosens. Bioelectron.* **90**, 410–417 (2017).
55. Caetano, L. P. *et al*. Carbon-nanotube Modified Screen-printed Electrode for the Simultaneous Determination of Nitrite and Uric Acid in Biological Fluids Using Batch-injection Amperometric Detection. *Electroanalysis* **30**, 1870–1879 (2018).
56. Czugala, M. *et al*. Portable integrated microfluidic analytical platform for the monitoring and detection of nitrite. *Talanta* **116**, 997–1004 (2013).


## Acknowledgements

This work was supported by the Applied Molecular Biosciences Unit-UCIBIO which is financed by national funds from FCT/MCTES (UID/Multi/04378/2013) and co-financed by the ERDF under the PT2020 Partnership Agreement (POCI-01-0145-FEDER-007728). C.M.S. and T.M. thank the financial support from Fundação para a Ciência e Tecnologia (Fellowships SFRH/BPD/79566/2011 and PD/BD/109687/2015). The authors acknowledge Dr. Isabel Moura for providing the nitrite reductase enzyme.

## Author Contributions

M.G.A. conceived the idea. C.M.S. and M.G.A. supervised the work. S.G. carried out the preliminary experiments. T.M. collected the data and wrote the manuscript. E.J. and L.A. fabricated and supplied the electrodes and provided critical insight to the experimental work. All authors reviewed and approved the manuscript.

## Additional Information

**Competing Interests:** The authors declare no competing interests.

**Publisher's note:** Springer Nature remains neutral with regard to jurisdictional claims in published maps and institutional affiliations.